# Propagation characteristics of biphotons in cold atomic vapor

**Chaoying Zhao (赵超樱)[1,2*] and Weihan Tan (谭维翰)[3]**

[1]*Department of Physics, College of Science, Hangzhou Dianzi University, Hangzhou 310018, China*
[2]*State Key Laboratory of Quantum Optics and Quantum Optics Devices, Institute of Opto-Electronics, College of Physics and Electronic Engineering, Shanxi University, Taiyuan 030006, China*
[3]*Department of Physics, College of Science, University of Shanghai, Shanghai 200444, China*
**Corresponding author: zchy49@hdu.edu.cn*

Received April 02, 2014; accepted June 18, 2014; posted online September 17, 2014

We investigate the propagation characteristics of the narrowband Stokes/anti-Stokes photons in cold atomic vapor. The four-wave mixing process results from parametric amplification of the anti-Stokes photons. We find that the process of parametric amplification is very similar to the light pulse propagating through an anomalous dispersion gain medium. Finally, we obtain the general solutions of the Glauber biphoton correlation functions, which are in good agreement with the experiment results.

*OCIS codes: 270.0270, 190.4410, 190.4380.*
*doi: 10.3788/COL201412.102701.*

In recent years, wide-band biphotons have received much attention due to their applications in quantum optics[1,2]. Usually, the entangled wide-band biphotons can be produced in a nonlinear crystal from spontaneous parametric downconversion[3–5]; however, the short coherence length of biphotons thus produced limits their application in long-distance quantum communication. Using a cold $^{87}$Rb atomic-gas media and electromagnetically induced transparency (EIT) assisted four-wave mixing (FWM) process[6–13], we generated the entangled narrowband biphotons experimentally in a double-$\Lambda$ system[14–19], in a two-dimensional magneto-optical trap[20,21], and in an optical cavity[22–25]. Usually, generation of narrowband biphotons is described using two approaches: the Heisenberg–Langevin method and the perturbation theory[14–19,26]. The biphoton source experiences two phases: 1) generation through the FWM process and 2) propagation in an atomic vapor. There are lots of experiment reports about the generation of biphotons; however, there are few reports about the propagation of biphotons. On the basis of these, we investigate the propagation characteristics of biphotons in atomic vapor in this letter. We find that the dynamic equations describing parametric amplification of the anti-Stokes photons are very similar to those of the light pulse propagating through an anomalous dispersion gain medium[27–29]. So, we adopt a similar method and obtain the solutions of the Glauber biphoton correlation function $G^{(2)}(\tau)$.

This letter is organized as follows: First, we discuss the propagation of light pulse through an anomalous dispersion medium. Second, we investigate the dynamic equations of the Stokes and anti-Stokes fields and their analytics solutions. Third, we present the numerical solutions of the Glauber biphoton correlation functions $G^{(2)}(\tau)$. Finally, we draw conclusions.

In Wang–Kuzmich–Dogariu experiment (the Ce vapor), the linear susceptibility $\chi(\omega)$ near the resonance frequency is[28]

$$\chi(2\pi\nu) = \frac{M}{\nu - \nu_0 - \Delta\nu + i\gamma} + \frac{M}{\nu - \nu_0 + \Delta\nu + i\gamma}, \quad (1)$$

which represents a medium with the spectral width $\gamma$ at resonance frequency $\nu_0$, where $\omega = 2\pi\nu$ and $M$ is related to the gain coefficient.

In FWM experiments (the $^{87}$Rb vapor), the linear susceptibility $\chi_{as}(\omega)$ near the atomic resonance frequency, when $\gamma_d/\Omega_e \ll 1$, is[17]

$$\chi_{as}(\omega) \simeq \frac{M}{\omega + i\gamma_e - (\Omega_e/2)} + \frac{M}{\omega + i\gamma_e + (\Omega_e/2)}, \quad (2)$$

where $M = -N\sigma_{13}\lambda_{13}\gamma_{13}/(4\pi)$, $N$ is the atomic density, $\sigma_{13} = 2\pi|\mu_{13}|^2/(\varepsilon_0\hbar\lambda_{13}\gamma_{13})$ is the on-resonance atomic absorption cross section, $\mu_{ij}$ are the electric dipole matrix elements, $\gamma_{ij}$ are the dipole relaxation rate, and $\gamma_e = (\gamma_{13} + \gamma_{12})/2$ is the effective relaxation rate. The effective coupling Rabi frequency is given by $\Omega_e = \sqrt{|\Omega_c|^2 - (\gamma_{13} - \gamma_{12})^2}$, where $\Omega_p = \mu_{14}E_p/\hbar$ and $\Omega_c = \mu_{23}E_c/\hbar$, respectively, are the pump and coupling laser Rabi frequencies with $E_p$ and $E_c$ as the complex amplitudes of the electric fields. The standard four-level double-$\Lambda$ EIT scheme with the generated anti-Stokes field is shown in Fig. 1.

The pump laser $\omega_p$ is applied to the atomic transition $|1\rangle \to |4\rangle$ with a detuning $\Delta_p = \omega_p - \omega_{41}$. A coupling laser $\omega_c$ tuned to $|2\rangle \to |3\rangle$ transition sets up

 

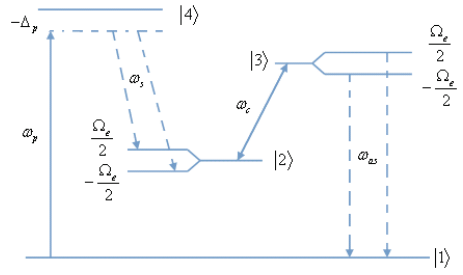


Fig. 1. Energy-level diagram for the double-Λ-type atoms.

a quantum interference and provides transparency for an anti-Stokes laser. To eliminate absorptive losses, the anti-Stokes light $\omega_{as}$ is driven by the spontaneous emission of Stokes light $\omega_s$ via the backward FWM process. These frequencies satisfy energy conservation $\omega_s = \omega_p + \omega_c - \omega_{as}$.

In frequency unit, substituting $\tilde{\omega} = \omega/2\pi$, $\tilde{\gamma}_e = \gamma_e/2\pi$, $\tilde{\Omega}_e = \Omega_e/2\pi$, and $m = M/2\pi$ in Eq. (2), we get

$$\chi_{as}(\tilde{\omega}) \simeq \frac{m}{\tilde{\omega} + i\tilde{\gamma}_e - (\tilde{\Omega}_e/2)} + \frac{m}{\tilde{\omega} + i\tilde{\gamma}_e + (\tilde{\Omega}_e/2)}. \quad (3)$$

We find that for $^{87}$Rb atomic vapor, Eq. (3) has the same form as Eq. (1) for Ce atomic vapor.

In case when pump beam absorption is small, i.e., $\Omega_p/\Delta_p \simeq 0.1 \ll 1$, the Raman gain can be ignored. The linear susceptibilities determine the natural spectral width and transmission spectrum of the generated anti-Stokes and Stokes fields passing through the medium. For instance, the EIT profile coefficient is

$$\Gamma_{as}(\omega) = -\frac{2iN\sigma_{13}\gamma_{13}(\omega + i\gamma_{12})}{(|\Omega_c|)^2 - 4(\omega + i\gamma_{13})(\omega + i\gamma_{12})}, \quad (4)$$

the nonlinear coupling coefficient is

$$\kappa_{as}(\omega) = \frac{\Omega_p}{\Delta_p}\frac{iN\sigma_{13}\gamma_{13}}{8}\frac{|\Omega_c|}{\Omega_e}\left(\frac{1}{\omega + i\gamma_e - (\Omega_e/2)} - \frac{1}{\omega + i\gamma_e + (\Omega_e/2)}\right), \quad (5)$$

and the Fourier transformation of Eq. (5) is

$$\tilde{\kappa}_{as}(\tau) = \frac{1}{2\pi}\int_{-\infty}^{\infty} e^{-i\omega\tau}\kappa_{as}(\omega)\mathrm{d}\omega = \frac{\Omega_p}{\Delta_p}\frac{N\sigma_{13}\gamma_{13}}{8}\frac{|\Omega_c|}{\Omega_e}e^{-\gamma_e\tau}\sin\left(\frac{\Omega_e}{2}\tau\right). \quad (6)$$

The weak-pulsed pump and strong continuous-wave coupling laser are considered as classical quantities and their interactions with the medium are described semiclassically. The generated Stokes and anti-Stokes fields are weak and thus are described quantum mechanically by operators $\hat{a}_{as}(\omega, z)$ and $\hat{a}_s^{\dagger}(\omega, z)$. Working in Heisenberg picture, ignoring the quantum Langevin noise operator $\hat{F}_{as}(z,\omega)$[14], the operators $\hat{a}_{as}(\omega, z)$ and $\hat{a}_s^{\dagger}(\omega, z)$ satisfy the following equation:

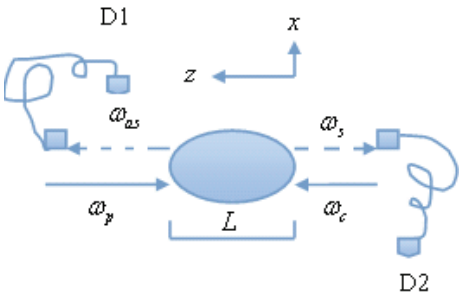


Fig. 2. Schematic for spontaneous backward-wave paired photon generation.

$$\frac{\partial \hat{a}_{as}}{\partial z} - \Gamma_{as}(\omega)\hat{a}_{as} = \kappa_{as}(\omega)\hat{a}_s^{\dagger}. \quad (7)$$

Let us look at the simple experiments of biphoton joint-detection measurement as shown in Fig. 2.

In Fig. 2, $L$ is the length of the EIT medium. Weak pump laser is first injected at the left surface ($z = L$), which produces the backward FWM process. Then strong coupling laser is injected at the right surface ($z = 0$). The final generated phased-matched Stokes and anti-Stokes photons propagate through the EIT medium, in the opposite directions, and go to detectors D1 and D2, respectively.

The general solutions are

$$\begin{aligned} &\hat{a}_{as}(z,\omega) = -\int_0^L \mathrm{d}z' e^{-\Gamma_{as}(\omega)(z-z')}\tilde{\kappa}_{as}(\tilde{\omega})\hat{a}_s^{\dagger}(z',\omega), && 0 \le z \le L \\ &\hat{a}_{as}(z,\omega) = g(\omega)e^{-\Gamma_{as}(\omega)L}\hat{a}_s^{\dagger}(L,\omega), && z \ge L \end{aligned}, \quad (8)$$

$$g(\omega) = \frac{-\int_0^L \mathrm{d}z' e^{\Gamma_{as}(\omega)z'}\hat{a}_s^{\dagger}(z',\omega)}{\hat{a}_s^{\dagger}(L,\omega)}\tilde{\kappa}_{as}(\tilde{\omega}) \simeq L\tilde{\kappa}_{as}(\tilde{\omega}). \quad (9)$$

We can easily see that the anti-Stokes light pulse is driven by the Stokes light pulse.

In time domain, the operators can be expressed as

$$\hat{a}_s^{\dagger}(z,t) = \frac{\int_{-\infty}^{\infty}\mathrm{d}\omega\hat{a}_s^{\dagger}(z,\omega)e^{i(k_s(\omega)z-\omega t)}}{\sqrt{2\pi}}, \quad (10)$$

$$\hat{a}_{as}(z,t) = \frac{\int_{-\infty}^{\infty}\mathrm{d}\omega\, g(\omega)e^{-\Gamma_{as}(\omega)z}\tilde{a}_s^{\dagger}(z,\omega)e^{i(k_{as}(\omega)z-\omega t)}}{\sqrt{2\pi}}. \quad (11)$$

The complex wavenumbers of Stokes and anti-Stokes photons satisfy $k_s(\omega) + k_{as}(\omega) = 0$, with the time delay $\tau = t_s - t_{as}$ between the detection of Stokes and anti-Stokes photons, we have $\int_{-\infty}^{\infty}\mathrm{d}t e^{-i(\omega+\omega')t}/2\pi = \delta(\omega + \omega')$. Considering the spontaneous emission Stokes light has resulted from zero-point oscillation of the electromagnetic field, and the pump light is of very short pulse,

the spectrum of the spontaneous emission Stokes light is flat. We take $\hat{a}_s^{\dagger}(z,\omega)\hat{a}_s(z,\omega) \approx \hat{a}_s^{\dagger}\hat{a}_s = n_s = 1/2$ [30].

The solution of the Glauber biphoton correlation function is given as

$$G^{(2)}(\tau) = \left| \frac{\int \mathrm{d}\omega T(\omega) e^{-i\omega\tau} e^{-\Gamma_{as}(\omega)L} L\tilde{\kappa}_{as}(\tilde{\omega})}{4\pi} \right|^2 . \quad (12)$$

The anti-Stokes light transmits across the boundary to the free space[31], so we have

$$T(\omega) = \frac{2n(\omega)}{1+n(\omega)} = \frac{\sqrt{1+\chi_{as}(\omega)}}{0.5+0.5\sqrt{1+\chi_{as}(\omega)}} . \quad (13)$$

We choose the following parameters: $N = 10^{11}\ \mathrm{cm}^{-3}$, $L = 10^{-3}$ m, $\lambda_{13} = 785$ nm, $M = -1.86\times10^{-3}\times2\pi$ MHz, $\gamma_{13} = 1.79\times10^{7}$ radians $= 3\times2\pi$ MHz, $\Delta_p = 7.5\gamma_{13}$, $\sigma_{13} = 10^{-9}\,\mathrm{cm}^2$, $\gamma_{12} = 0.6\gamma_{13}$, and $\Omega_p = 0.8\gamma_{13}$ [15]. The coupling laser Rabi frequency is $\Omega_{c1} = 23.4\gamma_{13}$, $\Omega_{c2} = 16.8\gamma_{13}$, $\Omega_{c3} = 8.4\gamma_{13}$, $\Omega_{c4} = 6.0\gamma_{13}$, and $\Omega_{c5} = 4.0\gamma_{13}$. Setting $\omega/2\pi = 0-300$ MHz and the time delay $\tau = 0-0.2\,\mu$s, we obtain the Glauber biphoton correlation function $G^{(2)}(\tau)$ as shown in Figs. 3 and 4.

With the increase in $\tau$, the curve damps quickly. In comparison with the experimental data in Ref. [14], the solid curve is in good agreement with the experimental results. We note that the two curves of the biphoton correlation functions disappear after $\tau = 0.142\,\mu$s.

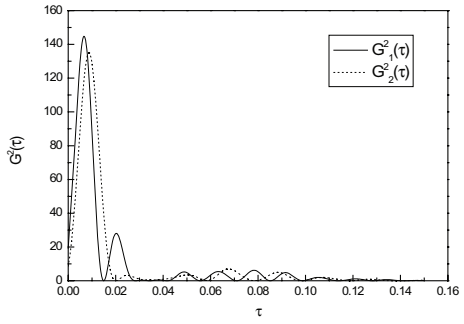


Fig. 3. 0–0.2 $\mu$s Biphoton correlation function $G_i^{(2)}(\tau)$, $i = 1,2$, $\Omega_{c1} = 23.4\gamma_{13}$, $\Omega_{c2} = 16.8\gamma_{13}$.

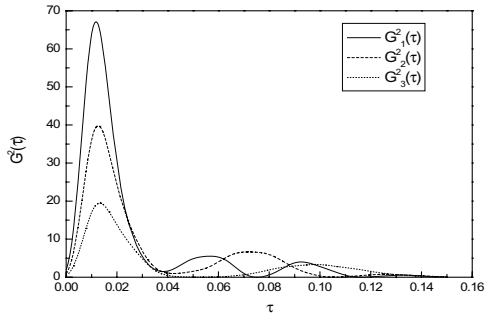


Fig. 4. Biphoton correlation function $G_i^{(2)}(\tau)$, $i = 1,2,3$, $\Omega_{c3} = 8.4\gamma_{13}$, $\Omega_{c4} = 6.0\gamma_{13}$, $\Omega_{c5} = 4.0\gamma_{13}$.

The biphoton correlation functions $G^{(2)}(\tau)$ depend on the coupling field Rabi frequencies $\Omega_c$. With the decrease in frequencies $\Omega_c$, the oscillations decrease. In case when $\tau = 0-0.065\,\mu$s, the three curves decline in orderly manner, whereas when $\tau = 0.065-0.173\,\mu$s, the three curves decline in disorderly manner. With the increase in the breadth of the first plate, the three curves experience three, two, and one fluctuation, respectively. After $\tau = 0.173\,\mu$s, the three curves disappear together, which approximately equals to the decay time constant $\tau_r = 1/2\gamma_{13} = 0.167\,\mu$s determined by the atomic natural linewidth.

In conclusion, on the basis of the dynamic equations of the generated Stokes and anti-Stokes photons, we discuss the case of $e^{-\Gamma_{as}(\omega)z} \neq 1$ and obtain the analytics solutions of the Glauber biphoton correlation function. At the same time, we assume the pump light is of very short pulse, therefore, the generated spontaneous emission Stokes light is also of very short pulse and its spectrum is nearly independent of frequency. The numerical calculation shows that the solution of the Glauber correlation function $G^{(2)}(\tau)$ is in good agreement with the experimental results.

This work was supported by the State Key Laboratory of Quantum Optics and Quantum Optics Devices, Shanxi University, Shanxi, China under Grant No. KF201401.

## References

1. Y. H. Shih, Rep. Prog. Phys. **66**, 1009 (2003).
2. D. N. Klyshko, *Photons and Nonlinear Optics* (CRC Press, New York, 1988).
3. A. Yoshizawa, D. J. Fukuda, H. D. Tsuchida, Opt. Commun. **313**, 333 (2014).
4. Y. Guo, W. Zhang, N. Lv, Q. Zhou, Y. D. Huang, J. D. Peng, Opt. Express **22**, 2620 (2014).
5. A. Christ, C. Lupo, M. Reichelt, T. Meier, C. Silberhorn, Phys. Rev. A **90**, 023823 (2014).
6. L. M. Duan, M. D. Lukin, J. I. Cirac, and P. Zoller, Nature **414**, 413 (2001).
7. S. Lioyd, M. S. Shahriar, J. H. Shapiro, and P. R. Hemmer, Phys. Rev. Lett. **87**, 167903 (2001).
8. H. de Riedmatten, I. Marcikic, W. Tittel, H. Zbinden, D. Collins, and N. Gisin, Phys. Rev. Lett. **92**, 047904 (2004).
9. S. E. Harris, Phys. Today **50**, 36 (1997).
10. B. Y. Wang, T. Wang, J. Tang, X. M. Li, and C. B. Dong, J. Appl. Phys. **115**, 023101 (2014).
11. T. Kampschulte, W. Alt, S. Manz, M. Dorantes, R. Reimann, S. Yoon, D. Meschede, M. Bienert, and G. Morigi, Phys. Rev. A **89**, 033404 (2014).
12. Y. Ma, J. Deng, Z. Hu, H. He, and Y. Wang, Chin. Opt. Lett. **11**, 022701 (2013).
13. Y. Ma, J. Deng, Z. Hu, H. He, and Y. Wang, Chin. Opt. Lett. **11**, 032701 (2013).
14. V. Balić, D. A. Braje, P. Kolchin, G. Y. Yin, and S. E. Harris, Phys. Rev. Lett. **94**, 183601 (2005).
15. P. Kolchin, S. W. Du, C. Belthangady, G. Y. Yin, and S. E. Harris, Phys. Rev. Lett. **97**, 113602 (2006).
16. P. Kolchin, Phys. Rev. A **75**, 033814 (2007).
17. S. W. Du, J. M. Wen, and M. H. Rubin, J. Opt. Soc. Am. B **25**, C98 (2008).

18. S. W. Du, J. M. Wen, M. H. Rubin, and G. Y. Yin, Phys. Rev. Lett. **98**, 053601 (2007).
19. S. W. Du, E. Oh, J. M. Wen, and M. H. Rubin, Phys. Rev. A **76**, 013803 (2007).
20. A. Kuzmich, W. P. Bowen, A. D. Boozer, A. Boca, C. W. Chou, L. M. Duan, and H. J. Kimble, Nature **423**, 731 (2003).
21. J. H. Li, R. Yu, L. G. Si, and X. X. Yang, J. Phys. B At. Mol. Opt. Phys. **43**, 065502 (2010)
22. J. M. Wen and M. H. Rubin, Phys. Rev. A **74**, 023808 (2006).
23. J. M Wen and M. H. Rubin, Phys. Rev. A **74**, 023809 (2006).
24. S. J. Yun, J. M. Wen, P. Xu, M. Xiao, and S. N. Zhu, Phys. Rev. A **82**, 063830 (2010).
25. H. J. Metcalf and P. van der Straten, *Laser Cooling and Trapping* (Springer, New York, 2002).
26. J. K. Thompson, J. Simon, H. Loh, and V. Vuletić, Science **313**, 74 (2006).
27. R. Y. Chiao, Phys. Rev. A **48**, R34 (1993).
28. L. J. Wang, A. Kuzmich, and A. Dogariu, Nature **406**, 277 (2000).
29. W. H. Tan, Q. Z. Guo, and Y. C. Meng, J. Opt. A Pure Appl. Opt. **10** 055004 (2008).
30. L. I. Schiff, *Quantum Mechanics* (McGraw-Hill, New York, 1968).
31. M. Born and E. Wolf, *Principles of Optics* (Pergamon, Oxford, 1975).